Elsevier Editorial System(tm) for Sensors & Actuators: B. Chemical

Manuscript Draft

Manuscript Number: SNB-D-07-00068R2

Title: A WIRELESS LC CHEMICAL SENSOR BASED ON A HIGH QUALITY FACTOR EIS CAPACITOR

Article Type: Research Paper

Keywords: Wireless sensor; chemical sensor; LC sensor; EIS capacitor, photoinjection

Corresponding Author: Dr Antonio Baldi,

Corresponding Author's Institution:

First Author: Jesus Garcia-Canton, BS

Order of Authors: Jesus Garcia-Canton, BS; Angel Merlos, Ph.D.; Antonio Baldi, Ph.D.

Abstract: This paper reports on the concept, design, fabrication and experimental results of a new passive wireless sensor for pH measurements. The sensor is based on a LC resonator formed by an inductor and an EIS (Electrolyte-Insulator-Silicon) capacitor working as a pH-to-capacitance transductor. A reference electrode is used to obtain a stable DC potential at the electrolyte. An additional comb-like electrode located on the surface of the insulator is also provided to obtain a low AC impedance. Using this double-electrode scheme a Q larger than 15 is achieved for a wide range of conductivities. Wireless measurements of the LC sensor yields a sensitivity of 1.0% frequency change per pH unit.

Figure 1
Click here to download high resolution image

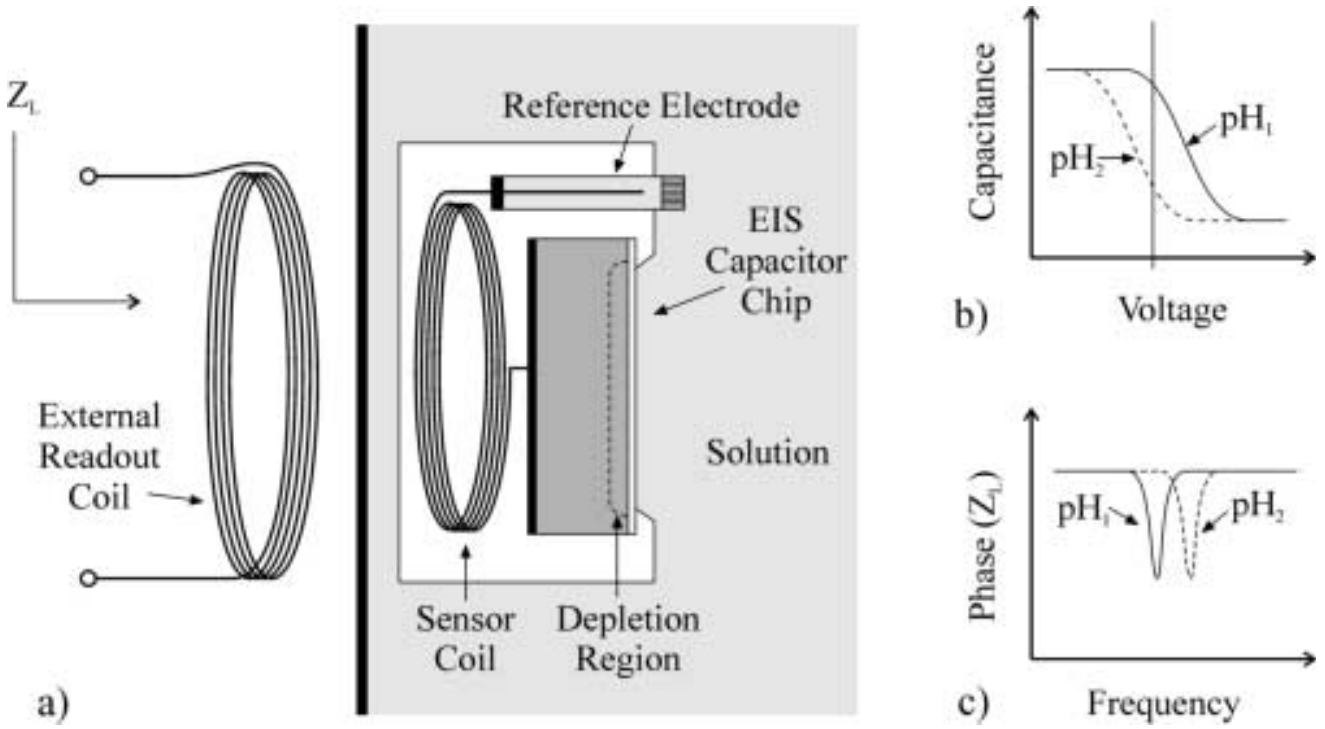

Figure 2
Click here to download high resolution image

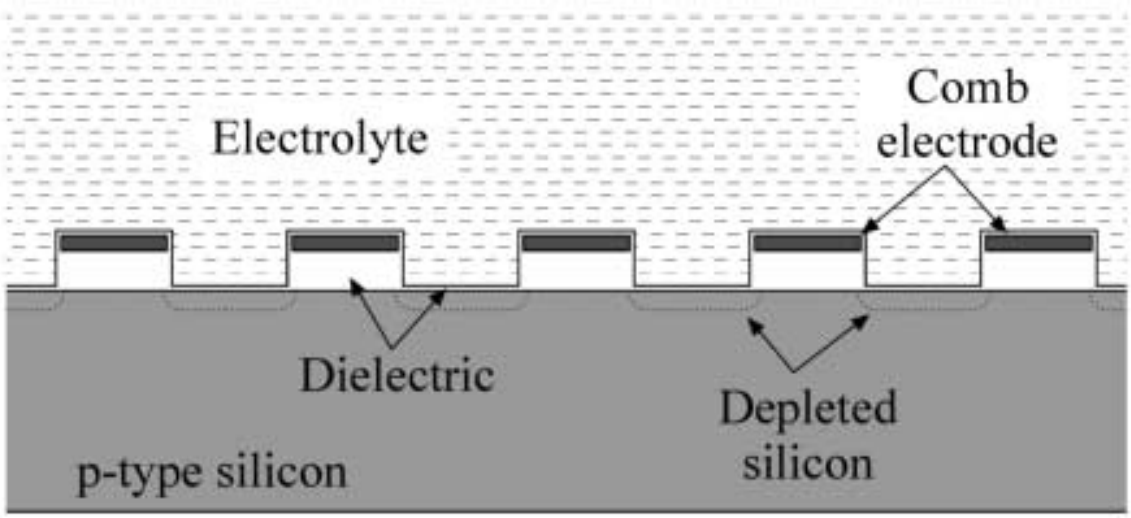

a)

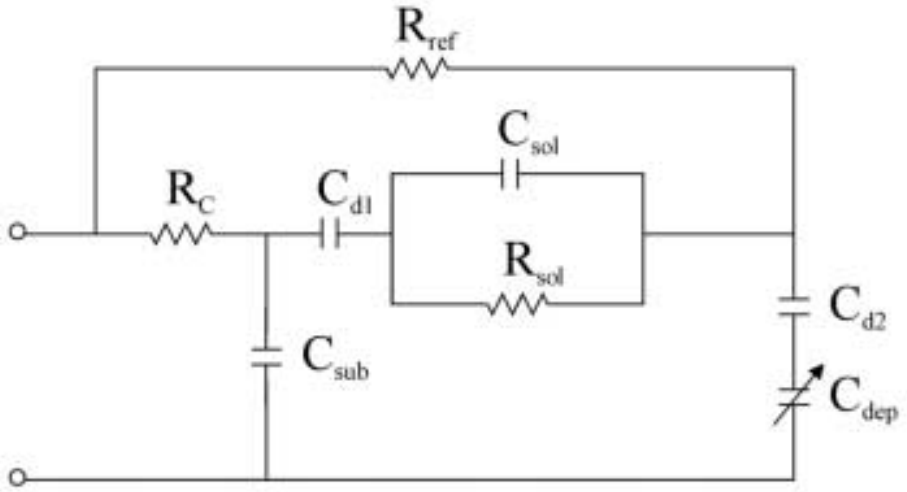

b)

Figure 3
Click here to download high resolution image

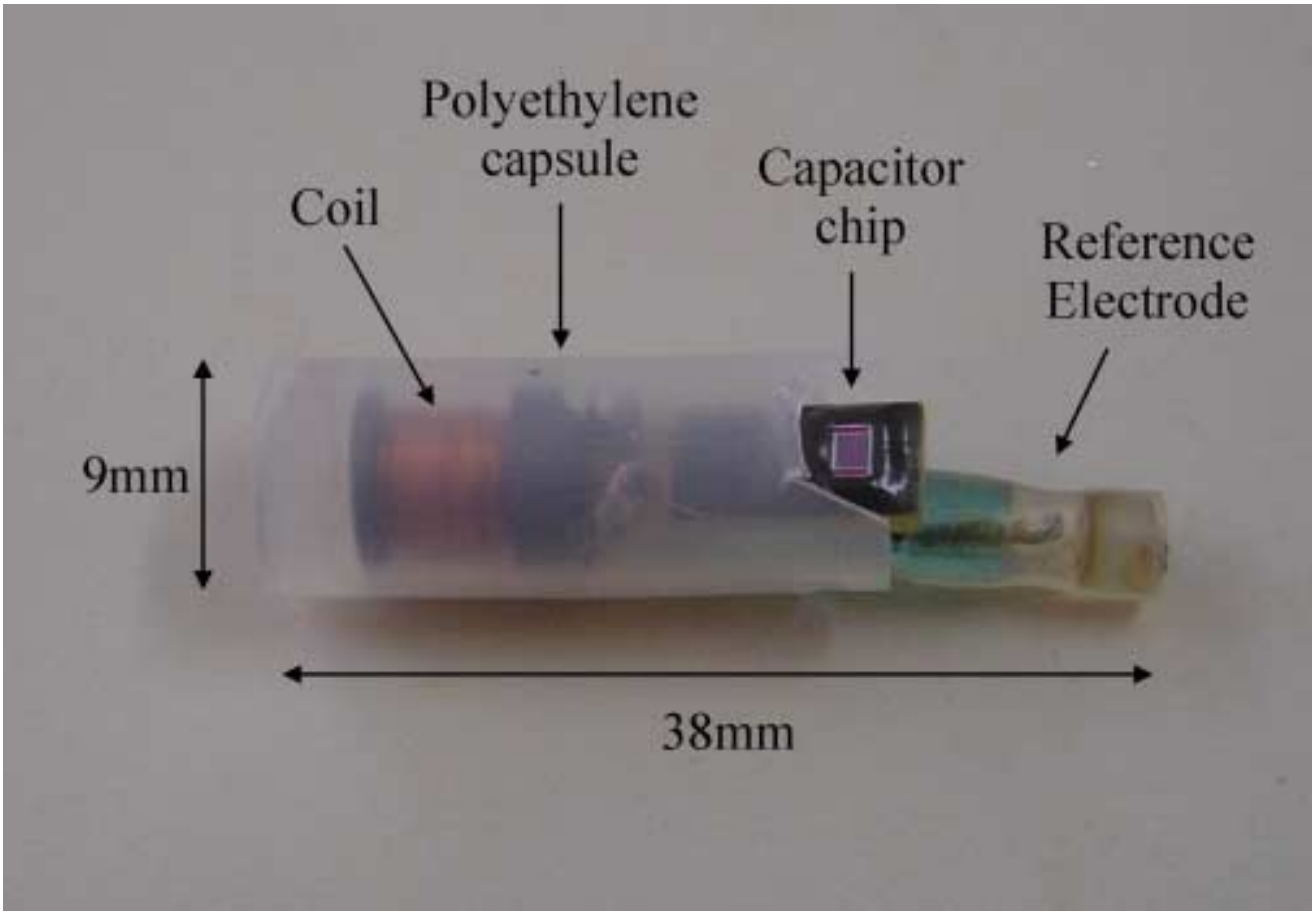

Figure 4
Click here to download high resolution image

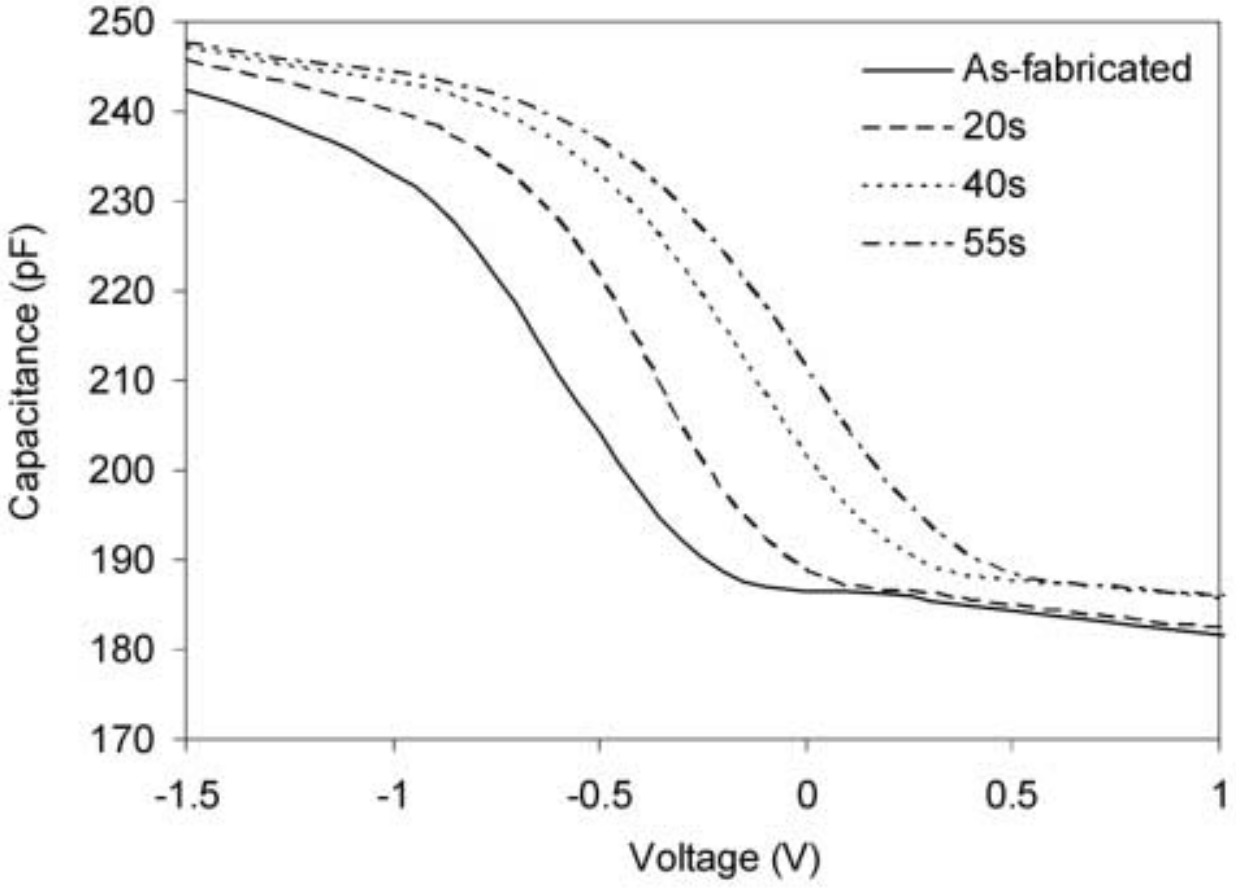

Figure 5
Click here to download high resolution image

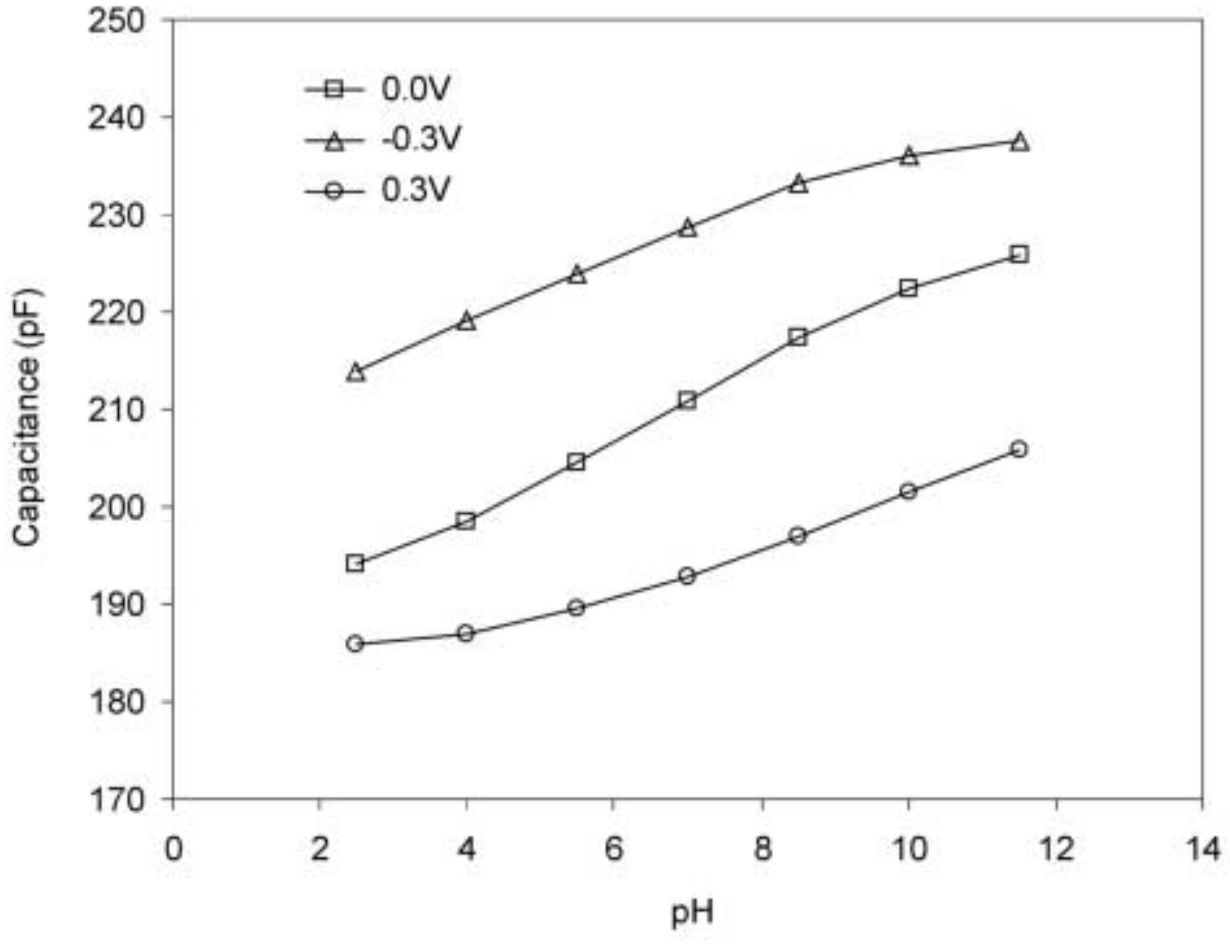

Figure 6
Click here to download high resolution image

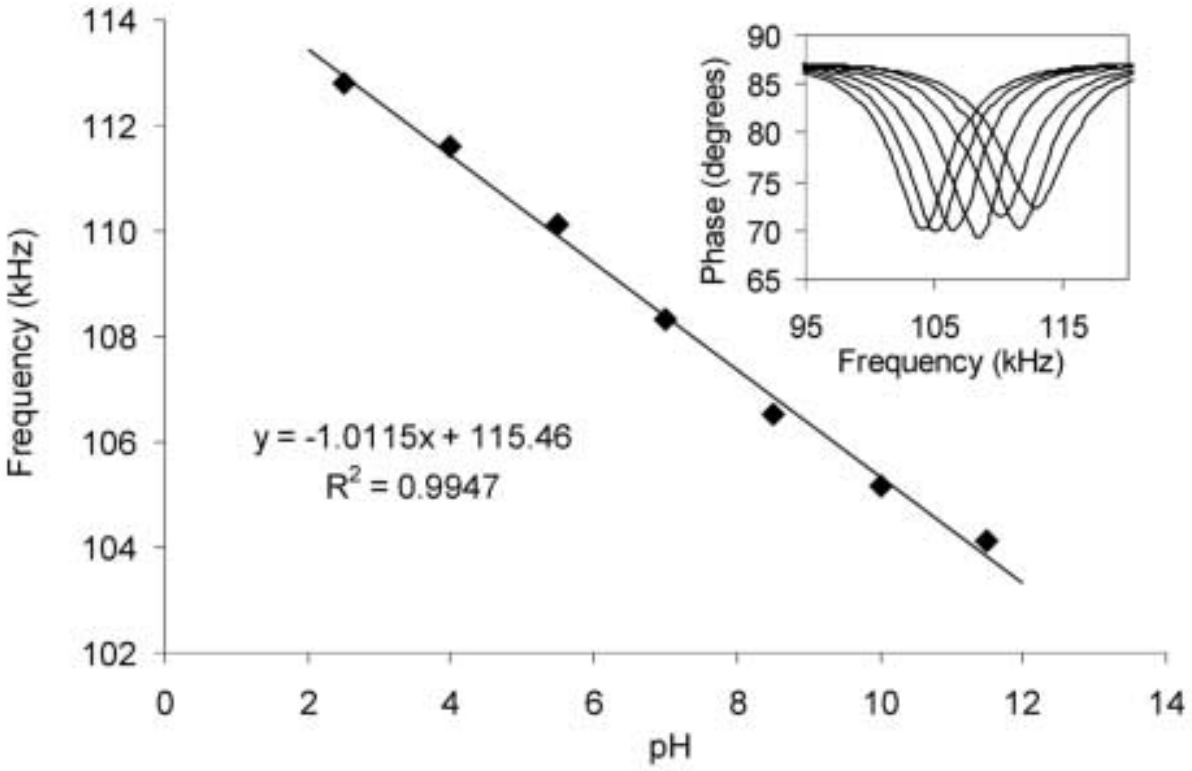

Figure 7
Click here to download high resolution image

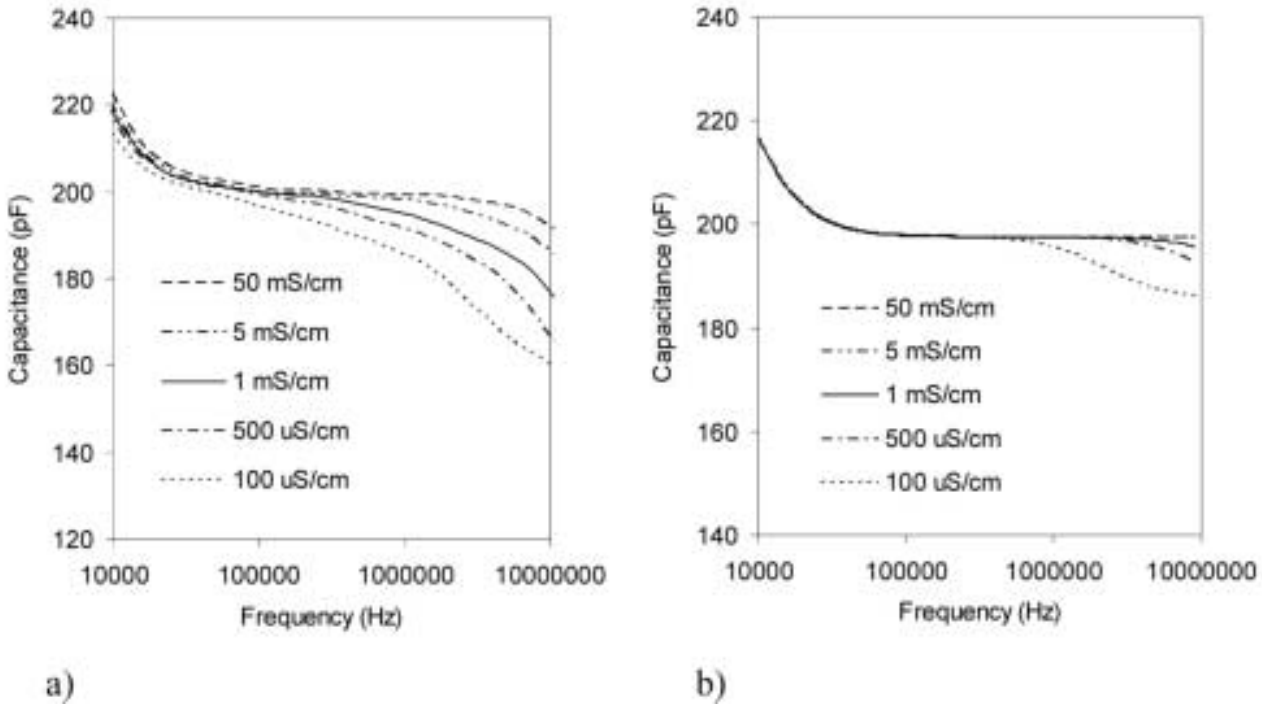

Figure 8
Click here to download high resolution image

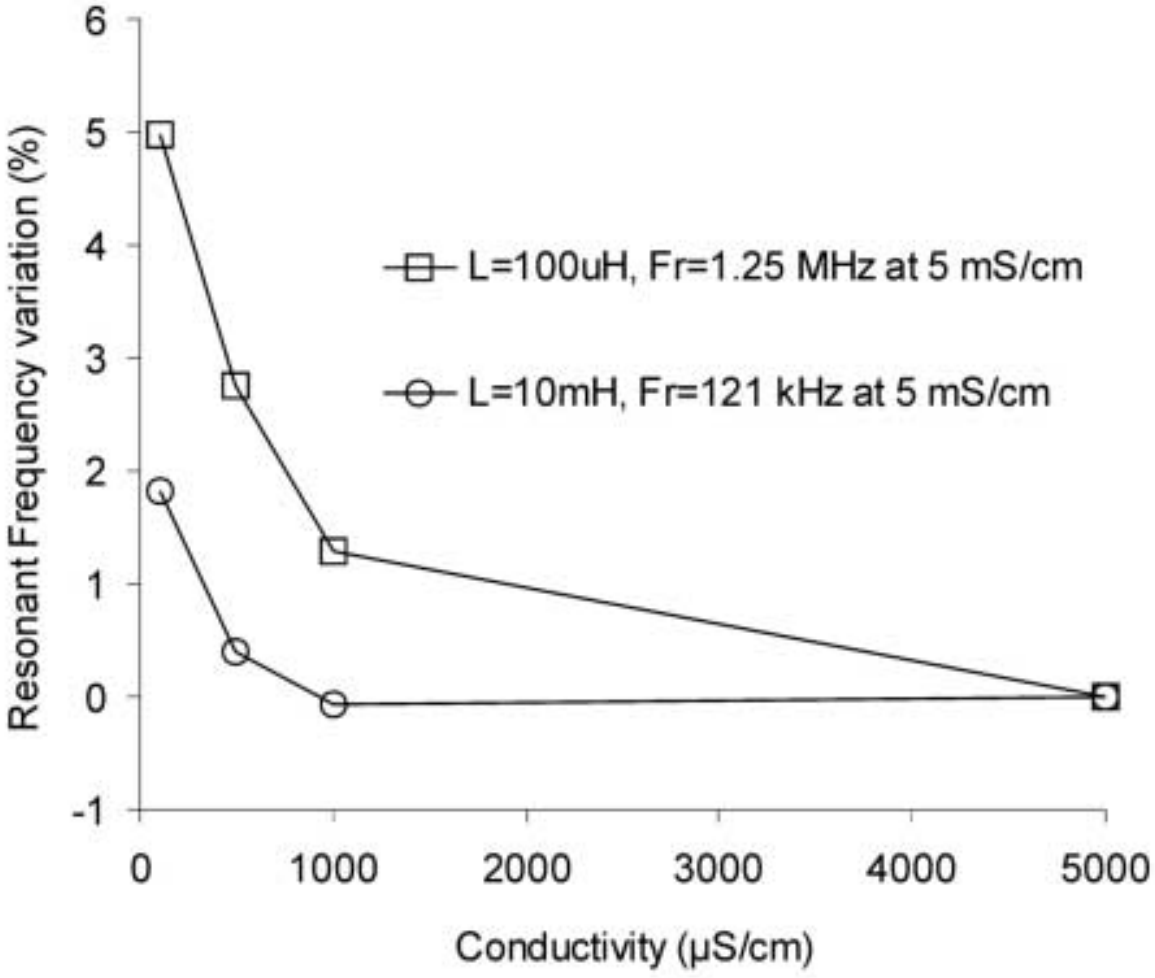

Figure 9
Click here to download high resolution image

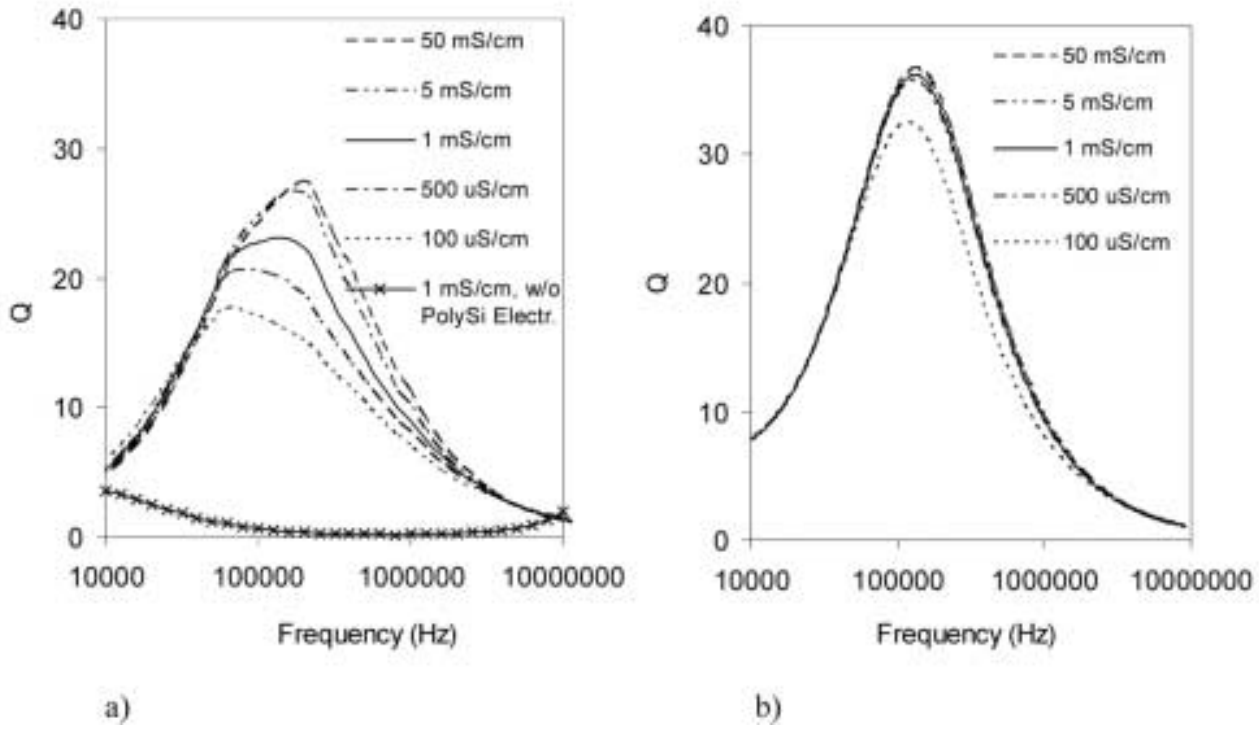

A WIRELESS *LC* CHEMICAL SENSOR BASED ON A HIGH QUALITY FACTOR EIS CAPACITOR

J. Garcia-Canton, A. Merlos, and A. Baldi

Centro Nacional de Microelectrónica-IMB (CSIC), Esfera UAB, E-08193 Cerdanyola, Spain.

ABSTRACT

This paper reports on the concept, design, fabrication and experimental results of a new passive wireless sensor for pH measurements. The sensor is based on a *LC* resonator formed by an inductor and an EIS (Electrolyte-Insulator-Silicon) capacitor working as a pH-to-capacitance transductor. A reference electrode is used to obtain a stable DC potential at the electrolyte. An additional comb-like electrode located on the surface of the insulator is also provided to obtain a low AC impedance. Using this double-electrode scheme a *Q* larger than 15 is achieved for a wide range of conductivities. Wireless measurements of the *LC* sensor yields a sensitivity of 1.0% frequency change per pH unit.

1. INTRODUCCTION

Short range wireless sensors are being developed for applications where monitoring physical or chemical parameters inside objects (e.g. bottled products, chemical reactors, or living beings) is necessary and the presence of electrical connections is not convenient. Currently, commercial wireless sensors are being used for monitoring purpose in biomedical and clinical applications [1]. These sensors include amplification and RF circuits, antenna and batteries. Passive wireless sensors are a simpler, cheaper, and battery-free alternative that could reach a wider range of applications. They are based on structures capable of absorbing or reflecting energy at a determined frequency. Different principles have been used to implement such sensors including surface acoustic waves [2], magnetoelastic effects [3] and *LC* resonator circuits [4-7]. *LC* sensors are based on the variation of capacitance, and

therefore of resonant frequency, in response to changes in the magnitude of interest. These sensors are attractive because of the easy of creating capacitors sensitive to different environmental parameters. Wireless readout of the sensor is achieved by measuring impedance changes at an external coil which is magnetically coupled to the sensor.

Most *LC* sensors found in the literature were designed to measure physical magnitudes [4, 5]. Chemical concentration measurements with *LC* sensors reported previously were based on stimuli-sensitive hydrogels [6, 7]. More recently, an *LC* chemical sensor based on an EIS (Electrolyte-Insulator-Silicon) capacitive structure was presented by the authors [8]. In the present paper various design aspects of these sensors will be addressed.

It is well known that EIS capacitors are sensitive to pH [9, 10]. A modification of the electrolyte pH results in a shift in its *C-V* curve. Therefore, a pH-to-capacitance transductor can be obtained by biasing the device with a suitable constant voltage. In the proposed wireless sensor an inductor is connected in parallel to the EIS capacitor, which implies 0 V DC biasing. Electrical connection to the electrolyte (i.e. the solution being measured) is provided by a reference electrode. Figure 1 is a simplified schematic representation of the sensor concept. In order to obtain a measurable sensor, certain aspects have to be considered when designing and fabricating it. For example, the quality factor of the resonator should be high and the *C-V* curve of the EIS capacitor should be centred at 0V for a pH-to-capacitance transduction to take place. These two important issues are addressed in the next section.

2. HIGH *Q* EIS CAPACITOR DESIGN AND MODELLING

A common technique for wireless measurement of the resonant frequency is based on detecting the local minimum of the impedance phase at an external readout coil. The depth of the phase dip at the resonant frequency can be approximated by

$$\Delta\varphi \cong \tan^{-1}(k^2 Q) \qquad (1)$$

where k is the coupling coefficient and Q is the quality factor of the sensor. From this equation is evident that the higher the Q, the deeper the phase dip, which should be easier to detect. A good quality factor also permits a longer measurement distance since a lower k is compensated by a higher Q in equation (1).

If we were to use the simplified scheme in Figure 1, the resistance of the reference electrode liquid junction (typically a few kΩ) and of the solution between the electrode and the EIS capacitor dielectric surface (also in the order of kΩ for low conductivity solutions) would prevent achieving high Q values. In order to overcome this problem we propose a double electrode scheme. The second electrode should be connected in parallel to the reference electrode and should have a low associated resistance at the resonant frequency. To avoid altering the stable potential provided by the reference electrode at DC a capacitor should be placed in series with the low resistance electrode.

Figure 2.a shows a cross-section of the double electrode EIS capacitor structure used in this work, which has been designed to meet the above mentioned requirements. The low resistance electrode consists of a set of polysilicon tracks that run parallel to and are interdigitated with another set of EIS capacitor strips. This geometry minimizes the resistance of the solution between the surface of the electrode and the surface of the capacitance dielectric. A double layer of silicon oxide and silicon nitride has been used as dielectric for the EIS capacitor. This double layer provides linear response to pH and has been extensively used in field effect chemical sensors [11, 12]. The same double layer isolates the polysilicon electrodes. In this fashion a capacitor is also formed between this electrode and the solution. Another thick dielectric layer underneath the polysilicon layer forms an additional direct capacitance to the substrate.

The equivalent circuit model of the above described EIS capacitor structure is shown in Figure 2.b. This circuit can be used to estimate the overall capacitance and resistance, and

hence, the quality factor of the structure. R_c and R_{ref} represent the resistance of the polysilicon traces and the resistance associated to the reference electrode, respectively. C_{d1} and C_{d2} are the capacitances of the dielectric layers between the polysilicon and the solution and between the solution and the silicon substrate, correspondingly. The solution is located in between these two capacitors, and is modelled as a resistor in parallel with a capacitor (R_{sol} and C_{sol}). The capacitance of the thick oxide underneath the polysilicon traces is represented by C_{sub}. Finally, the variable capacitance of the silicon depletion layer is represented by C_{dep}. The values for R_c, C_{sub}, C_{d1}, C_{d2}, and C_{dep} are calculated from geometrical parameters, whereas the values for R_{sol}, and C_{sol} are obtained from simulation with electromagnetic finite element analysis software (MAXWELL2D, Ansoft corp.). In the design presented here the polysilicon traces are 3 µm wide, 0.45 µm high and 1600 µm long and separated from the substrate by a 0.8 µm-thick oxide. Distance between traces (center to center) is 6 µm. The EIS capacitance areas between each two pair of fingers are therefore 3 µm wide and 1600 µm long. A total 218 electrode fingers form a 1.6 mm x 1.8 mm sensitive area. Using the equivalent circuit described above one can estimate that a high Q is theoretically achieved for a wide range of frequencies with this design, as will be shown in Section 5.

Besides the quality factor requirements, another issue that has to be addressed is the control of the flat band voltage of the EIS capacitive structure. In order to obtain a change in capacitance when the pH is modified, the depletion interval of the *C-V* curve, which is the portion of the curve with high slope, has to include 0 V for the whole pH range. This portion of the *C-V* curve for a MOS (Metal-Oxide-Silicon) capacitor can be approximated by the expression [13]

$$C = C_O\left[1+\frac{2K_O^2\varepsilon_0(V-V_{FB})}{qK_S t_O^2(N_A-N_D)}\right]^{-1/2} \qquad (V_{FB} < V < V_T) \qquad (2)$$

where ε_0 is the free space permittivity, q is the electronic charge, N_A and N_D are the donor and acceptor doping concentration of the substrate, V_{FB} is the flat band voltage, V_T is the threshold voltage, K_S C_O, K_O, and t_O are the oxide layer capacitance, relative permittivity and thickness, respectively. In the case of an EIS capacitor with an oxide-nitride double dielectric layer, t_O can be replaced by the equivalent oxide thickness

$$t'_O = t_O + t_N \frac{K_S}{K_N} \tag{3}$$

where K_N and t_N are the nitride layer relative permittivity and thickness, respectively. It is clear from Equation (2) that the position of the depletion interval in the *C-V* curve respect to the voltage axis depends on the flat band voltage, V_{FB}. In turn, the flat band voltage depends on other physical and chemical parameters [14]

$$V_{FB} = E_{Ref} - \psi_O + \chi^{sol} - \frac{\Phi_{Si}}{q} - \frac{Q_T}{C_O} \tag{4}$$

where E_{Ref} is the reference electrode potential, Ψ_O is the pH-dependent surface potential, χ^{sol} is the surface dipole potential of the solution, Φ_{Si} is the silicon electron work function, and Q_T is the total equivalent charge trapped in the dielectric layers and at the oxide-silicon interface states. The depletion interval of the *C-V* curve spans from V=V_{FB} to V= V_T. The threshold voltage, V_T, is given by

$$V_T = V_{FB} + 2\phi_F + \frac{1}{C_O}\sqrt{4qN_A K_S \varepsilon_0 \phi_F} \tag{5}$$

where ϕ_F is the Fermi potential. An EIS structure with a negligible density of trapped charge has a slightly negative V_{FB} (-410 mV for a p-type wafer, silicon oxide dielectric, pH 2.2 and a calomel reference electrode [15]) and a slightly positive V_T (420 mV for a 1000 Å-thick oxide on a $5 \cdot 10^{14}$ cm^{-1} p-type doped wafer as calculated with Equation (5)). Therefore, the requirement of a centred *C-V* curve is satisfied with common doping concentration and dielectric thickness, provided that the dielectric charge density is sufficiently low that it does

not affect significantly the flat band voltage. However, in the case of an oxide-nitride double dielectric layer it is difficult to avoid accumulation of charge during fabrication process due to a high density of charge traps [16]. As a consequence, much more negative flat band voltages, and hence the high slope of the *C-V* curve away from 0 V, may result. In order to solve this problem we can take advantage of the photoinjection effect [16], that is, irradiating the capacitive structure with UV light while applying low voltages across it.

As already mentioned, the useful voltage range of the *C-V* curve corresponds to the depletion interval. The depletion interval is given by

$$\Delta V_d = V_T - V_{FB} = 2\phi_F + \frac{t'_O}{K_O \varepsilon_0}\sqrt{4qN_A K_S \varepsilon_0 \phi_F} \qquad (6)$$

This interval must be larger than the foreseen changes in V_{FB} due to variations of pH. The maximum possible change in V_{FB} is about 800 mV for aqueous solutions, although a more reasonable value would be 550 mV (10 pH units and sensitivity of 55 mV/pH). From Equation (6) one could conclude that large t'_O and N_A values are desirable for a wide depletion voltage interval. However, a trade-off has to be made between range and sensitivity, since the latter is inversely proportional to t'_O and N_A, as shown in the expression of the maximum slope of the *C-V* curve defined in Equation (2)

$$\left.\frac{\partial C}{\partial V}\right|_{V=V_{FB}} = -\frac{K_O^3 \varepsilon_0^2}{qK_S t_O'^3 (N_A - N_D)} \qquad (7)$$

Another aspect to be taken in account is that low silicon doping for achieving high sensitivity has the negative effect of increasing the series resistance of the structure. Using high conductivity wafers with a low doping epitaxial top layer can solve this problem.

3. FABRICATION

Starting wafers have less than 0.02 ohm·cm resistivity with a 22.5 µm-thick epitaxial top layer of 26 ohm·cm ($5 \cdot 10^{14}$ cm^{-1}). A 0.8 µm-thick oxide is grown and a 0.45 µm-thick

polysilicon layer is deposited and doped. A single photolithography step is used to pattern the polysilicon and the oxide layers by reactive ion etch. Subsequently, a thin oxide layer is grown (780 Å) and a 1000 Å-thick nitride layer is deposited by LPCVD (Low Pressure Chemical Vapour Deposition). The fabrication is finished with front and back metalization and deposition and patterning of a PECVD (Plasma Enhanced Chemical Vapour Deposition) oxide passivation layer.

Once the wafers have been diced, individual chips are glued and wire-bonded to a PCB strip. Epotek H-70E epoxy resin is used to protect the wirebonds, the chip edges and the PCB tracks. The devices are then connected to a ferrite-core coil and a miniaturized Ag/AgCl reference electrode. The liquid junction of the reference electrode is a piece of Vycor® porous glass mounted in a short segment of rubber tube that can be easily pulled out from the electrode, so that replacement of the internal KCl solution is made possible. The whole assembly is introduced in a polyethylene capsule and filled with Sylgard 184 silicone (Figure 3). The EIS capacitors are irradiated with UV light (254 nm, 0.4 mW/cm^2) for a few seconds to center their *C-V* curves previously to the connection with the coil. The capacitors are immersed in pH 7 buffer and a voltage of 5 V is applied between the substrate and the solution during the irradiation.

4. EXPERIMENTAL

Measurements of response to pH were carried out in a universal buffer consisting of 0.04 M boric acid, 0.04 M acetic acid, and 0.04 M phosphoric acid, and 0.1 M KNO_3 as background electrolyte. The pH was adjusted by addition of 1 M NaOH. The *C-V* curves were measured with a HP4192 impedance analyser connecting the substrate to the low level input and the reference and polysilicon electrodes to the high level input. The response of the complete *LC* sensor to pH was wirelessly measured with a 15 turn, 2.5 cm diameter readout

coil at 1 cm from the sensor coil. The readout coil terminals were connected to the impedance analyser and the sensor resonant frequency was determined as the frequency at the minimum of the phase dip.

Curves of capacitance vs. frequency to study the effect of conductivity were also obtained with the HP4192 impedance analyser. Connection of the EIS structure to the analyser was carried out as in the *C-V* measurements. Solutions of different conductivity and constant pH were prepared by diluting a pH 7 buffer (from Crison Instruments, SA) or adding KCl to it. The pH was measured after preparation to ensure that the original value was maintained.

5. RESULTS AND DISCUSSION

The EIS capacitors were measured before UV irradiation, and after irradiation at fixed time intervals. Figure 4 shows the corresponding *C-V* curves. The high slope portion of the curve was located between -1 V and -0.25 V for the as-fabricated devices. Therefore, there was no pH sensitivity at 0 V biasing voltage for those devices. The results show how the *C-V* curve could be shifted laterally to the desired position by controlling the irradiation time. The change in V_{FB} of the structure is associated with the excitation of electrons in the valence band of silicon with energy high enough to overcome the potential barrier of the oxide and subsequent trapping in the nitride layer [16].

When exposed to solutions of different pH the EIS capacitor behaved as expected and shifts of the *C-V* curves corresponding to a quasi-Nernstian response (55 mV/pH) were obtained. The pH 7 curve was centred at 0 V and a fairly linear capacitance-to-pH response was obtained for this voltage, as shown in Figure 5. The effect of non-centred curves was estimated by obtaining the capacitance-to-pH response at positive or negative bias voltages, which resulted in less linear responses.

Figure 6 show the response of the complete *LC* wireless sensor to pH. The sensor exhibited a sensitivity of 1.0 kHz per pH unit, which corresponds to a 1.0 % frequency change per pH unit. The linearity of the response is not significantly affected by the quadratic relation between capacitance and frequency. This is due to the fact that the total capacitance change is only about 10% of the central capacitance.

The effect of solution conductivity on the sensor response was studied both experimentally and by simulation. The interference of salt concentration on the electrochemical response of the nitride-electrolyte interface was considered negligible, as demonstrated for other field-effect chemical sensors using nitride gate [17]. Therefore, only the effect of conductivity on the EIS structure impedance was studied. Figures 7.a and 7.b show the measured and simulated capacitances, respectively, for different solution conductivities in the 10kHz to 10MHz frequency range. Simulations were carried out with PSPICE using the equivalent circuit in Figure 2.b. Perfect matching of the equivalent circuit model with the experimental data is not possible due to the distributed nature of the capacitances and resistances of the solution and the electrodes. Even so, a reasonable prediction of the conductivity effect is achieved with the model. The effect of conductivity at high frequencies comes from the fact that the solution behaves as a parallel RC circuit with variable cutoff frequency depending on the solution conductivity. At low frequency the solution behaves as a resistance. At high frequencies the solution behaves as a capacitance in series with the dielectric and depletion capacitances, and therefore the total capacitance is reduced. The increase in capacitance seen at lower frequencies can be associated to the reference electrode. At those frequencies the impedance of the polysilicon-to-solution capacitor, C_{dl}, is comparable to the impedance associated to the reference electrode. In order to avoid AC currents going through the reference electrode, and hence, degrading the quality factor, its impedance was deliberately increased with a 100 kΩ series resistor. From both

experimental and simulated curves one can observe that the region of lower conductivity effect is located around 100 kHz. The resonant frequency vs. conductivity curves for two *LC* sensors working at 121 kHz and 1.27 MHz, shown in Figure 8, also confirm a lower conductivity effect at lower frequencies.

Finally, the quality factor of the EIS capacitor was measured for different solution conductivities. As shown in Figure 9.a, the *Q* is high for a wide range of conductivities and frequencies. Measurement of *Q* for an EIS capacitor with no connection to the polysilicon electrode, that is, using only the reference electrode, yields a much lower *Q*. This confirms the necessity of the polysilicon electrode to obtain a high *Q*. Moreover, the effect of solution conductivity is much larger when the polysilicon electrode is not used (results not shown). The results of simulation with the equivalent circuit model, shown in Figure 9.b, agree well with the experimental curves. The lower measured *Q* is probably due to a higher-than-expected resistivity of the polysilicon.

6. CONCLUSION AND OUTLOOK.

The feasibility of using an EIS capacitive structure as a pH sensitive capacitor for *LC* wireless sensors was demonstrated. A sensitivity to pH of 1.0% frequency change per pH unit was obtained. The *Q* of the *LC* resonator was high for any solution conductivity thanks to the use of a low impedance comb-like polysilicon electrode in addition to the reference electrode. Response to conductivity could be minimized by selecting a suitable working frequency. However, the present sensor design has a considerable sensitivity to conductivity below 500μS/cm. One possible approach to reduce this undesired sensitivity is the minimization of the contribution of the solution impedance to the total impedance. This could be achieved by reducing the spacing and width of the polysilicon traces. Another drawback of the device presented here is the necessity of adjusting its flat band voltage at the packaged device level. Possible solutions

are the use of other dielectric materials with less charge-trap densities or the optimization of the current dielectric layer thickness to minimize the effect of trapped charges (e.g. a thicker SiO_2 and a thinner Si_3N_4 layer). The optimization of the *C-V* curve to achieve a higher sensitivity and higher linearity will also be considered in the future.

ACKNOWLEDGEMENTS

This work is supported by the Plan Nacional de Investigación Científica, Desarrollo e Innovación Tecnológica 2004-2007 of the D.G.I.-S.G.P.I (TEC2004-00068). The authors wish to thank Mr. Alberto Moreno and Mr. Hector Cabezas for PCB encapsulation of the sensors, and Alfredo Cadarso for technical support in the photoinjection experiments. The devices presented in this paper were fabricated at the IMB-CNM Clean Room.

REFERENCES

[1] J.E. Pandolfino, Bravo capsule pH monitoring, American Journal of Gastroenterology 100 (2005) 8-10.

[2] W. Buff, S. Klett, M. Rusko, J. Ehrenpfordt, M. Goroli, Passive remote sensing for temperature and pressure using SAW resonator devices, IEEE Trans. Ultrasonics, Ferroelectrics and Frequency Control, 45 (1998) 1388-1392.

[3] Q. Y. Cai and C. A. Grimes, A remote query magnetoelastic pH sensor, Sensors & Actuators B, Chem., 71 (2000) 112–117.

[4] K. G. Ong, C. A. Grimes, C. L. Robbins and R. S. Singh, Design and application of a wireless, passive, resonant-circuit environmental monitoring sensor, Sensors and Actuators A, 93 (2001) 33-43.

[5] M.A. Fonseca, J.M. English, M. von Arx, M.G. Allen, Wireless micromachined ceramic pressure sensor for high-temperature applications**,** Journal of Microelectromech. Syst., 11 (2002) 337-343.

[6] M. Lei, A. Baldi, Tingrui Pan, Yuandong Gu, Ronald A. Siegel, and Babak Ziaie, "A hydrogel-based wireless chemical sensor", MEMS'04 Technical Digest, Maastricht, The Netherlands, Jan. 25-29, 2004.

[7] Z.A. Strong, A.W. Wang, and C.F. McConaghy, Hydrogel-actuated capacitive transducer for wireless biosensors, Biomedical Microdevices 4 (2002) 97-103.

[8] J. Garcia-Canton, A. Merlos, A. Baldi, High-Quality Factor Electrolyte Insulator Silicon Capacitor for Wireless Chemical Sensing, IEEE Electron Device Letters 28 (2007) 27-29.

[9] M. J. Schöning, D. Tsarouchas, L. Beckers, J. Schubert, W. Zander, P. Kordos and H. Lüth, A highly long-term stable silicon-based pH sensor fabricated by pulsed laser deposition technique, Sensors and Actuators B, Chemical, 35 (1996) 228-233.

[10] M.J. Schöning, N. Näther, V. Auger, A. Poghossian and M. Koudelka-Hep, Miniaturised flow-through cell with integrated capacitive EIS sensor fabricated at wafer level using Si and SU-8 technologies, Sensors and Actuators B, Chem., 108 (2005) 986-992.

[11] D. Harame, L. Bousse, J. Schott and J. Meindl, Ion-sensing devices with silicon nitride and borosilicate glass insulators, IEEE Trans. Electron Devices, 34 (1987) 1700-1706.

[12] T. Yoshinobu, H. Ecken, A. Poghossian, H. Lüth, H. Iwasaki and M. J. Schöning, Alternative sensor materials for light-addressable potentiometric sensors, Sensors and Actuators B, Chem., 76 (2001) 388-392.

[13] R.F. Pierret, Field effect devices, Modular Series on Solid State Devices, vol. 4, Ed. Addison-Wesley Publishing Company, Reading, 1983, p. 49.

[14] P. Bergveld, A. Sibbald, Analytical and biomedical applications of ion-selective field-effect transistors, Elsevier, Amsterdam, 1988, p. 13.

[15] L. Bousse, Single electrode potentials related to flat-band voltage measurements on EOS and MOS structures, J. Chem. Phys., 76 (1982) 5128-5133.

[16] V.J. Kapoor, R.A. Turi, Charge storage and distribution in the nitride layer of the metal-nitride-oxide-semiconductor structures, J. Appl. Phys., 52 (1981) 331-319.

[17] S. Alegret, J. Bartroli, C. Jimenez, M. del Valle, C. Dominguez, E. Cabruja, and A. Merlos, pH-ISFET with NMOS Technology, Electroanalysis, 3 (1991) 355-360.

FIGURE CAPTIONS

Figure 1: a) Schematic representation of the wireless chemical sensor concept, b) typical response of the EIS capacitor to a pH change, and c) phase of the readout coil impedance.

Figure 2: a) Cross-sectional representation of the EIS capacitor with polysilicon comb electrode, and b) equivalent circuit model of the EIS capacitor.

Figure 3: Encapsulated sensor.

Figure 4: C-V curves of as-fabricated and UV-irradiated EIS structures.

Figure 5: Capacitance vs. pH at three different bias voltages.

Figure 6: Response of the pH wireless sensor. Inset shows the phase curves measured at the readout coil.

Figure 7: a) Measured and b) simulated capacitance of the EIS structure at different conductivities.

Figure 8: Measured response of the wireless pH sensor to conductivity for two working frequencies.

Figure 9: a) Measured and b) simulated Q of the EIS structure at different conductivities. The Q of an EIS structure measured without connecting the polysilicon electrode is also included in a).

BIOGRAPHIES

Jesús García-Cantón received his BS degree in Industrial Engineering from the Universitat Politècnica de Catalunya, (2004). Afterwards, he joined the Chemical Transducers Group at the Centro Nacional de Microelectronica (CNM) in Barcelona, Spain. He is actually a PhD student and he is working in the field of solid state microelecrodes and wireless passive chemical sensors.

Angel Merlos was born in Sabadell (Barcelona), Spain, in 1965. He received the Ph.D. degree in 1993 from the Autonomous Universisty of Barcelona. In 1988 he joined the Nano and Microsystems Departmentat the Instituto de Microelectronica de Barcelona, CNM-IMB(CSIC). His areas of interest include microsystems technologies and their applications to integrated sensors and actuators.

Antonio Baldi received his BS degree in Telecommunication Engineering from the Universitat Politècnica de Catalunya in 1996. He did research on chemical microsensors at the Centro Nacional de Microelectrónica in Barcelona (CNM-IMB, CSIC) for five years until he received his PhD degree on Electronics Engineering from the Universitat Autònoma de Barcelona in 2001. From 2001 to 2003 he was at the University of Minnesota, working in the field of bioMEMS as a postdoctoral fellow. In the summer of 2003 he joined the Chemical Transducers Group, at the Centro Nacional de Microelectrónica, where he works on the development of microsystems and instrumentation for chemical and biochemical sensing as a "Ramon y Cajal" researcher.